

LOOKING BACK AT FORTY YEARS OF TEACHING AND  
RESEARCH IN LUDWIG PRANDTL'S HERITAGE OF BOUNDARY  
LAYER FLOWS

by

**J.L. van Ingen**

39th Ludwig Prandtl Memorial Lecture,

Prague

28 May 1996

ZAMM Zeitschrift Angewandte Mathematik und Mechanik 78  
(1998) 1. 3-20

Note: Teaching and research in aerodynamics at an aerospace engineering faculty should show a strong interaction between fundamental aspects and its application in design. The lecture illustrates this by discussing a number of research topics of the author's group in relation to airfoil design for low speed applications.

ZAMM · Z. Angew. Math. Mech. **78** (1998) 1, 3–20

INGEN, J. L. VAN

## Looking Back at Forty Years of Teaching and Research in Ludwig Prandtl's Heritage of Boundary Layer Flows

39th Ludwig Prandtl Memorial Lecture, Prague, 28 May 1996<sup>1)</sup>

*Lehre und Forschung auf dem Gebiete der Aerodynamik an einer Fakultät für Luft- und Raumfahrt soll eine starke gegenseitige Wechselwirkung zeigen zwischen Grundlagen und Anwendung im Entwurf. Die Vorlesung erläutert dies durch die Behandlung einiger Untersuchungen im Labor des Autors zum Entwurf von Flügelprofilen für die Anwendung bei niedrigen Geschwindigkeiten.*

*Teaching and research in aerodynamics at an aerospace engineering faculty should show a strong interaction between fundamental aspects and its application in design. The lecture illustrates this by discussing a number of research topics of the author's group in relation to airfoil design for low speed applications.*

MSC (1991): 76-03, 76D10

### 1. Introduction

Although the lecture will be in English, it is appropriate to start with a few words in German to express my gratitude for having been invited to present the 39th Ludwig Prandtl Memorial Lecture.

Den Vorständen von DGLR und GAMM möchte ich – in PRANDTL's eigener Sprache – ganz herzlich danken für die von mir sehr hochgeschätzte Einladung, die 39. Ludwig-Prandtl-Gedächtnis-Vorlesung zu halten. Für jeden, der in der Mechanik und besonders auf dem Gebiete der Grenzschichten gearbeitet hat, ist es eine sehr große Ehre, in die Reihen der Fachgenossen aufgenommen zu werden, die vorher diese Gedächtnis-Vorlesung gehalten haben. Ich hoffe, daß der heutige Vortrag einiges dazu beitragen kann, das Leben und Schaffen von LUDWIG PRANDTL zu ehren. Dazu ist es angemessen, mit den Beziehungen zwischen PRANDTL und Delft zu beginnen.

I came to Delft in 1949 as a first year student in the Faculty of Aeronautical Engineering. This Faculty had been founded in 1940, but of course a real start had only been made in 1945. Later the name of the Faculty has been changed into Aerospace Engineering. In 1949 there were two full professors: H. J. VAN DER MAAS, teaching flight mechanics, and A. VAN DER NEUT, teaching aircraft structures. Applied aerodynamics was taught by senior lecturer E. DOBBINGA. Theoretical Fluid Dynamics was taught by J. M. BURGERS and Solid State Mechanics by C. B. BIEZENO and W. T. KOITER, all from the Faculty of Mechanical Engineering. From 1960 onwards theoretical aerodynamics was taught within the Faculty of Aeronautical Engineering itself by J. A. STEKETEE, a former student of J. M. BURGERS. Both BIEZENO and BURGERS had been appointed in Delft at a very young age (BIEZENO in 1914 at the age of 26 and BURGERS in 1918 at the age of 23). BURGERS had been invited to the newly established chair in Aero- and Hydrodynamics, while still being a Ph.D. student of EHRENFEST in Leiden (see [2]).

It should be remembered that the First International Congress of Applied Mechanics was organized at Delft in 1924 by BIEZENO and BURGERS together with PRANDTL, VON KÁRMÁN, GRAMMEL, and others, after a preparatory meeting at Innsbruck in 1922. This meeting in Delft laid the foundation for what later has become IUTAM. Since PRANDTL died in 1953 and I finished my engineering study in 1954, I never had the privilege of meeting him personally. As is the case with most people of my age, the name of PRANDTL became known to me through studying aerodynamic subjects such as wing theory and above all boundary layer theory. As a student I had taken courses in boundary layer theory from BURGERS and TIMMAN. I had the privilege of following some post graduate lectures from BURGERS in 1954 while he was still struggling with the equation which later was named after him.

During his introductory lectures in applied aerodynamics DOBBINGA showed us the "Prandtl film" in which various viscous flow phenomena and the process of the generation of vortices were shown. This film had come to Delft from the National Aeronautical Laboratory (later NLR) which apparently had received it from PRANDTL himself in the early 30's. A description of this film is given in [3], which is based on two publications by PRANDTL himself [4, 5]. Still pictures from this film are of course known to numerous generations of students in fluid dynamics through the famous PRANDTL-TIETJENS volumes<sup>2)</sup>.

From 1956 on I was charged, as an assistant at the Faculty of Aeronautical Engineering, with teaching a course on boundary layers. I have been teaching this course during 40 years now and I can say that I enjoyed every hour of it. Of course my inspiration during the development of this course was found in PRANDTL's publications, such as his

<sup>1)</sup> This paper gives an abridged version of the lecture; a more extensive version will be made available as [1]

<sup>2)</sup> Since it appeared that hardly anybody in the audience had ever seen this film, it was shown in full at the end of the lecture

contribution to DURAND and of course in SCHLICHTING's book. I have witnessed the development of the subject from the time where a practical application of boundary layer theory was only possible through the use of Pohlhausen type methods, to the present day where I can demonstrate to my students a rather complicated boundary layer computation on a PC in the lecture room. I have, however, always tried to put emphasis on understanding of the subject above brute force of computation.

Because teaching and performing research in the field of boundary layer flows, a world which has been opened up to me by the writings of PRANDTL, has given me such an immense satisfaction during my working life, I have chosen as the title for this 39th Prandtl Memorial Lecture: "Looking back at 40 years of teaching and research in LUDWIG PRANDTL's heritage of boundary layer flows".

During my work at Delft I have always taken the view that teaching and research in aerodynamics at an aerospace engineering faculty should show a strong interaction between fundamental aspects and its application in design. In my lecture I will illustrate this by discussing a number of research topics of our group in relation to airfoil design for low speed applications. Another way to dedicate our work to PRANDTL's memory is to discuss some results on 3-D wings, vortices, flow visualization, and experimental techniques. Due to lack of time and space this discussion will have to be rather fragmentary. Since most of my own work has been on low speed aerodynamics, the present lecture will emphasize incompressible flow.

## 2. Teaching two-dimensional incompressible laminar boundary layer computation

Of course it was only through the genius of PRANDTL that the calculation of laminar boundary layers came in sight when he in 1904 simplified the Navier-Stokes equations to the boundary layer equations. For an orthogonal curvilinear coordinate system in two-dimensional flow these equations read as follows:

$$u \frac{\partial u}{\partial x} + v \frac{\partial u}{\partial y} = U \frac{dU}{dx} + \nu \frac{\partial^2 u}{\partial y^2}; \quad \frac{\partial u}{\partial x} + \frac{\partial v}{\partial y} = 0 \quad (1)$$

with boundary conditions

$$u = v = 0 \quad \text{at} \quad y = 0; \quad u \rightarrow U(x) \quad \text{for} \quad y \rightarrow \infty. \quad (2)$$

Note that the shape of the body only enters through the pressure gradient term  $U (dU/dx) = -(1/\rho) (dp/dx)$ , which is assumed to be known when calculating the boundary layer. When inserting the boundary conditions at the wall into (1) we obtain the "first compatibility condition at the wall" relating the curvature of the velocity profile at the wall to the pressure gradient.

In the beginning of this century it was still too complicated to calculate the boundary layer for arbitrary pressure distributions. Hence at first only similar flows could be calculated, such as the flat plate (PRANDTL 1904, BLASIUS 1908), the plane stagnation point (HIEMENZ 1911) and the wedge-type flows (FALKNER-SKAN 1930; HARTREE 1937; and the reversed flow solutions by STEWARTSON in 1954<sup>3</sup>). Non-similar solutions could be obtained for special pressure distributions where the partial differential equations (1) could be reduced to a series of ordinary differential equations (BLASIUS 1908, HOWARTH 1935, GÖRTLER 1952). All of these series solutions failed to converge properly near separation and hence some kind of continuation procedure had to be devised which was either based on the momentum integral equation of VON KÁRMÁN (HOWARTH 1941, TANI 1949) or on a direct numerical solution (HARTREE 1939, LEIGH 1955). This work, especially that of HARTREE, led to the notion of a singularity at separation. Later on this singularity was clarified by GOLDSTEIN (1948) and STEWARTSON (1958), a further numerical evaluation was given by TERRILL (1960).

At first these discussions of the singularity gave rise to the idea that the boundary layer equations ceased to be valid at separation. Later on it has become clear that the boundary layer equations can be used through separation for a suitable pressure distribution, but that the result is extremely sensitive to small changes in the pressure distribution. Instead of prescribing the pressure distribution one should prescribe a regular behaviour through separation of a quantity such as the skin friction or the displacement thickness (MANGLER and SMITH 1959) from which the pressure distribution follows. At present it is customary to use the concept of "strong interaction" where the boundary layer is calculated simultaneously with the pressure distribution. Both are coupled through the distribution of the displacement thickness.

Until 1921 boundary layer theory was not of much use to practical aerodynamicists. This is illustrated by the fact that it was only in 1922 that BURGERS, during a visit to VON KÁRMÁN at Aachen, heard about the practical application of boundary layer theory through the use of the von Kármán momentum integral equation and the Pohlhausen method, based on it. Hence for a long time the practical application of boundary layer theory was through approximate methods such as POHLHAUSEN's (1921). It was only in the sixties that direct numerical calculations became feasible, see for instance SMITH and CLUTTER (1963).

<sup>3</sup>) Well known references, which can be found in the 7th edition of SCHLICHTING [6], ROSENHEAD [7], or VAN INGEN [21] will not be listed in this paper

In my lectures at Delft I discuss the laminar boundary theory in a mixture of the classical approach for similar flows and series solutions, such as found in Schlichting and a direct numerical approach. The solution of the boundary layer equations is complicated through the occurrence of boundary conditions at both ends of an, in principle, infinitely long interval between the wall and the edge of the boundary layer. Using a numerical initial value method, such as Runge-Kutta or a Taylor series method, requires the use of a "shooting procedure" where an additional boundary condition at the wall is guessed (e.g. the wall shear stress) and successively refined until the boundary condition at the edge of the boundary layer is satisfied.

Instead of the shooting method also a finite difference method can be used in which the boundary conditions at both ends of the interval are satisfied at the same time. For the finite difference method it appears to be sufficient to discuss the numerical solution algorithm for only one second-order linear ordinary differential equation with non-constant coefficients. This standard form is

$$\bar{u}'' + P(\eta) \bar{u}' + Q(\eta) \bar{u} = R(\eta) \quad (3)$$

with boundary conditions

$$\bar{u} = 0 \quad \text{at} \quad \eta = 0; \quad \bar{u} = \bar{u}_{\max} \quad \text{at} \quad \eta = \eta_{\max} (\rightarrow \infty), \quad (4)$$

where  $\bar{u}$  represents the non-dimensional velocity in the boundary layer. For certain applications where the exact solution is known, the exact value for  $\bar{u}_{\max}$  at a finite  $\eta_{\max}$  is used in order to be able to evaluate the quality of the numerical procedure. Equation (3) is solved in two ways:

- a 3-point finite difference method with application of the Thomas algorithm to solve the resulting linear algebraic equations,
- a 5-point finite difference method, which is only a little bit more complicated than the 3-point method, but much more accurate for the same steplength.

A first example is the asymptotic suction boundary layer ([6], chapter 14) for which we obtain  $\bar{u}'' + \bar{u}' = 0$  and hence  $P(\eta) = 1$ ;  $Q(\eta) = 0$ ;  $R(\eta) = 0$ . The exact solution is

$$\bar{u} = 1 - \exp(-\eta).$$

The second example is Stokes' first problem (accelerated infinite flat plate, [6], chapter 5). Writing this problem in a frame of reference where the wall is stationary and the outer flow is moving we find

$$\bar{u}'' + 2\eta\bar{u}' = 0; \quad P(\eta) = 2\eta; \quad Q(\eta) = 0; \quad R(\eta) = 0.$$

Because of the known exact solutions, the preceding examples can be used by the students to get some feeling for the influence of varying  $\eta_{\max}$  and the number of steps through the boundary layer and of course also for the merits of the various solution procedures.

The Blasius solution for the flat plate is described by an equation for the non-dimensional stream function  $f$  ([6], chapter 7)

$$f''' + \frac{1}{2} ff'' = 0 \quad \text{with} \quad f = 0, \quad f' = 0 \quad \text{at} \quad \eta = 0; \quad f' \rightarrow 1 \quad \text{for} \quad \eta \rightarrow \infty. \quad (5)$$

Equation (5) can easily be solved by the shooting method using the Taylor series and the Runge-Kutta method. The equation can also be solved by the finite difference method by bringing it into the form of our standard equation (3) by substituting  $f' = \bar{u}$  which leads to

$$\bar{u}'' + \frac{1}{2} f \bar{u}' = 0.$$

Apparently we have to take  $R = 0$  and  $Q = 0$  while  $P(\eta) = \frac{1}{2} f$ . This is a complicating factor because now  $P(\eta)$  is not known and the equation is not linear anymore. This problem is solved by using an iterative procedure where  $f$  is obtained from a previous iterate  $\tilde{u}$  using

$$f = \int_0^\eta \tilde{u} \, d\eta,$$

and taking  $\tilde{u} = 1 - \exp(-\eta)$  as a first estimate for  $\bar{u}$ . A few iterations using the 3-point or the 5-point scheme are found to be sufficient.

The Falkner-Skan equation in the well known Hartree form ([6], chapter 9) for the non-dimensional streamfunction  $f$  and its boundary conditions read

$$f''' + ff'' + \beta(1 - (f')^2) = 0; \quad f = f' = 0 \quad \text{at} \quad \eta = 0; \quad f' \rightarrow 1 \quad \text{for} \quad \eta \rightarrow \infty.$$

This equation allows repeated differentiations and hence the Taylor series method can be used in addition to the Runge-Kutta method for a shooting procedure. The use of the finite difference method is complicated by the occurrence of two non-linear terms  $ff''$  and  $(f')^2$ .

The first one is treated as in the Blasius equation, the second one is linearized using

$$f' = \bar{u}, \quad \bar{u} - \tilde{u} = \delta u, \quad (\delta u)^2 \approx 0,$$

where  $\tilde{u}$  is the value of  $\bar{u}$  from a previous iteration. This results in

$$\bar{u}'' + f\bar{u}' + (-2\beta\tilde{u})\bar{u} = -\beta(1 + \tilde{u}^2),$$

and hence

$$P(\eta) = f; \quad Q(\eta) = -2\beta\tilde{u}; \quad R(\eta) = -\beta(1 + \tilde{u}^2).$$

Again an iterative solution is easily obtained from  $f = \int_0^\eta \tilde{u} d\eta$  and a first guess  $\tilde{u} = 1 - \exp(-\eta)$ .

Non-similar boundary layers can be calculated from a form of the boundary layer equation which to a large extent resembles the Falkner-Skan equation. See for instance SMITH and CLUTTER (1963). However, in this case a partial differential equation results because derivatives of  $f$  and  $f'$  with respect to  $x$  occur. The equation has the advantage that for  $x \rightarrow 0$  the Falkner-Skan equation is obtained, hence the starting solution is known already. A marching procedure in  $x$ -direction can be obtained by replacing the derivatives with respect to  $x$  by finite differences based on a few points in  $x$ -direction (Hartree-Womersley method). The resulting ordinary differential equation in  $\eta$  can be solved by the shooting method (using the Runge-Kutta procedure) or can be brought in the standard form (3) using the same procedures as for the Falkner-Skan equation. As in all direct numerical calculations singular behaviour near separation is observed. A good estimate for the position of separation is obtained by assuming that the singularity is of the simple Goldstein type where the shear stress approaches zero as the square root of the distance to separation. Hence a linear extrapolation of the square of the shear stress seems to be sufficient. For practical purposes the more elaborate singularity description, as given by STEWARTSON is not necessary. The author demonstrates the various solution procedures in the classroom using a PC with overhead projection on a screen.

### 3. On the use of the method of integral relations to calculate laminar boundary layers

As was mentioned in the previous chapter, it is rather easy to calculate laminar boundary layers for arbitrary pressure distributions, using a direct numerical approach. Nevertheless the use of the method of integral relations is still discussed in the author's course. On the one hand this is done because of historical reasons and its educational value. On the other hand the better methods of integral relations are still useful in design procedures. For an optimal design of an airfoil it may be necessary to perform a great number of boundary layer calculations where the short computation time outweighs the disadvantage of a slightly lesser accuracy. Furthermore for airfoil design it is useful to have a method of integral relations with a one-parameter or preferably a two-parameter family of velocity profiles for which the results of stability calculations are available to be used in the  $e^n$  method for transition prediction (chapter 5). Also, if we want to calculate through separation using the method of strong interaction, an integral relation method offers advantages with respect to speed of calculation.

In my lectures I still discuss the Pohlhausen method (1921) in the version of HOLSTEIN and BOHLEN (1942). Basically in this method it is assumed that all velocity profiles can be represented by a fourth degree polynomial where all parameters except one are determined from boundary conditions and the first compatibility condition at the wall. The one remaining parameter results in a one-parameter family of velocity profiles; this parameter is then determined as a function of  $x$  from an ordinary differential equation for which the von Kármán momentum integral relation is used. With the following definitions

$$m = -\frac{\theta^2}{\nu} \frac{dU}{dx}, \quad l = \frac{\tau_0 \theta}{\mu U}, \quad H = \frac{\delta^*}{\theta}, \quad F = 2l + 2m(2 + H), \quad (6)$$

the momentum integral relation reduces to

$$\frac{d}{dx} \left( \frac{\theta^2}{\nu} \right) = \frac{F}{U}. \quad (7)$$

Due to the one-parameter family concept, all parameters mentioned under (6) are determined by one parameter for which any one of the set (6) can be used. Often  $F$  is considered to be a function of  $m$ . It was noted by WALZ (1941) and TANI (1941) and later by THWAITES (1949) that  $F(m)$  can be approximated by the linear relation  $F(m) = a + bm$  which leads to the following solution of the momentum integral relation (7):

$$\frac{U\theta^2}{\nu} = \frac{a}{U^{b-1}} \int_0^x U^{b-1} dx.$$

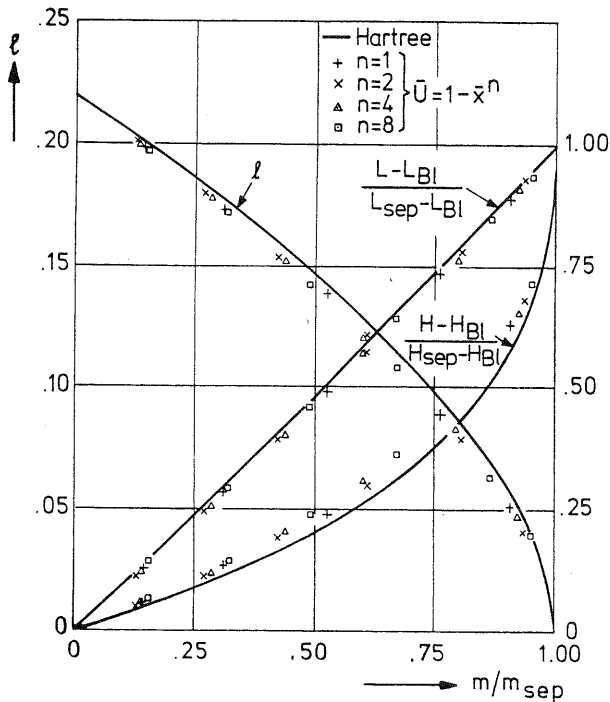


Fig. 1. Scaled boundary layer parameters as a function of  $m/m_{sep}$ . BL = Blasius; sep = separation

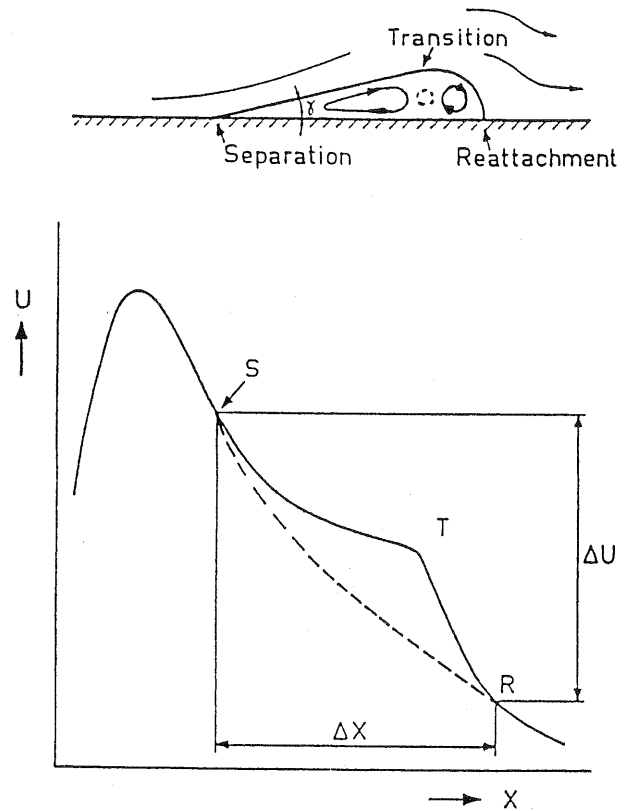


Fig. 2. Schematic picture of a separation bubble and pressure distribution

This simple relation for the momentum loss thickness  $\theta$  appears to be remarkably accurate; it has been used by THWAITES (1949) to derive his well known method. Although one-parameter methods can give an accurate estimate of  $\theta$ , it turns out that the shape of the velocity profiles and hence the position of separation can be rather inaccurate. It was shown by TANI (1954), HEAD (1957), CURLE [8], and the present author [9], that a two-parameter method would be sufficiently accurate for all engineering applications. As an example Fig. 1 shows that the characteristic parameters of a number of boundary layers can be collapsed on single curves if plotted vs  $m/m_{sep}$ , where  $m_{sep}$  is the value of  $m$  at separation [9]. It was shown by TANI (1954) and especially by CURLE [8] that a suitable second parameter (in addition to  $(\theta^2/\nu) (dU/dx) = -m$  is

$$n = \left( \frac{\theta^2}{\nu} \frac{dU}{dx} \right)^2 U \frac{d^2U}{dx^2} = \frac{\theta^4}{\nu^2} U \frac{d^2U}{dx^2}.$$

Note that  $n$  only depends on  $\theta$  and  $U(x)$ , since  $\theta$  can already be determined with good accuracy from a one parameter method (such as Thwaites'), it may be expected that a two-parameter method can be developed without having to employ a second differential equation.

#### 4. On the laminar part of separation bubbles

Laminar separation can occur on airfoils at low Reynolds numbers (e.g. sailplane wings and windturbine blades) but also at higher Reynolds numbers near the leading-edge of wings at high angles of attack. At very low Reynolds numbers laminar separation can be followed by laminar reattachment (see section 7), but in practice the more usual case is that the separated flow becomes turbulent and may or may not reattach (bubble bursting).

In sections 2 and 3 we have seen that the calculation of laminar separation may present difficulties due to the Goldstein singularity, which occurs in accurate numerical procedures, while the usual methods of integral relations may not be accurate enough near separation. Since in our work on airfoil design we needed a method to predict the characteristics of laminar separation bubbles we have performed extensive research on laminar separation [9–13].

Fig. 2 shows a typical pressure distribution for an airfoil with a separation bubble. Between laminar separation (S) and transition (T) the pressure distribution flattens due to the large displacement thickness in the bubble. Between

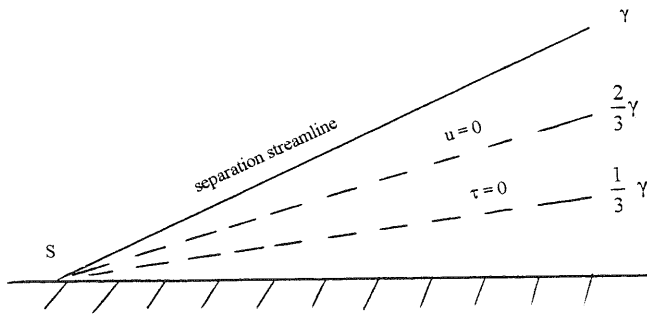


Fig. 3. Separation according to Legendre-Oswatitsch

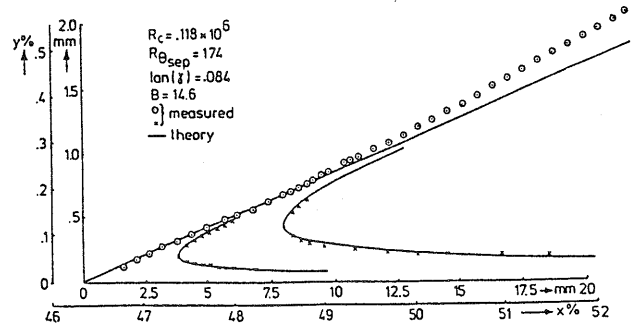


Fig. 4. Streamlines obtained from smoke picture.  $\odot \times$  experiments; — eq. (8)

transition (T) and reattachment (R) the turbulent flow shows a substantial pressure recovery. In the present section we will concentrate on the laminar part of the bubble.

To develop an integral relation method for the calculation of laminar separated flow we needed more information on separation than is given by the Goldstein singularity. In fact this singularity should not occur in real flows. An interesting description of laminar separation is due to LEGENDRE [14] and OSWATITSCH [15]. From a Taylor series development around a point of zero skin friction it follows that the separation streamline should leave the wall at an angle  $\gamma$  (Fig. 3) where  $\gamma$  and the streamlines are given by

$$\tan(\gamma) = -3 \frac{d\tau_0}{dx} \bigg/ \frac{\partial p}{\partial x}, \quad y^2(x \tan \gamma - y) = \text{const.} \quad (8)$$

Furthermore it follows that the points  $u = 0$  are on the straight line under an angle  $\frac{2}{3}\gamma$ , the zero skin friction line is under  $\gamma/3$ , and the pressure gradient vector is also under  $\gamma/3$ .

Since in practice  $\gamma$  is only of the order of a few degrees, the pressure gradient normal to the wall remains small and hence it may be expected that the boundary layer equations remain useful. In fact the relations (8) also follow from the boundary layer equations with, of course the exception of  $\text{grad}(p)$  which is assumed parallel to the wall [10–13]. It is clear from (8) that a boundary layer calculation with prescribed pressure distribution for which the Goldstein singularity occurs would lead to the unrealistic result  $\gamma = \pi/2$ .

An extensive series of flow visualization experiments was performed from which the angle  $\gamma$  was determined, it appeared that the streamlines obtained from smoke pictures corresponded well to equation (8). Fig. 4 shows an example. It appeared that a good correlation existed between  $\gamma$  and the Reynolds number based on  $U$  and the momentum-loss thickness  $\theta$  at separation (Fig. 5). Based on these experimental results a simple one-parameter method was developed using the momentum integral equation and the first compatibility condition at the wall. The Hartree-Stewartson profiles provided the closure relations; a prescribed shape of the separation streamline was used instead of the prescribed pressure distribution. This method was able to give a reasonable description of the laminar part of the bubble (for further details see [9–13]).

At a later moment it was tried to validate our experimental observations by a direct numerical approach based on the ideas on interaction of VELDMAN [16]. A famous example is the CARTER and WORNOM trough [17], where a flat plate is given a shallow indentation (Fig. 6). Cases for  $\alpha = -0.03$  and  $-0.05$  have been calculated by HENKES [18] and more recently by MEULEMAN [19]. The effect of the indentation and of the displacement thickness is taken into

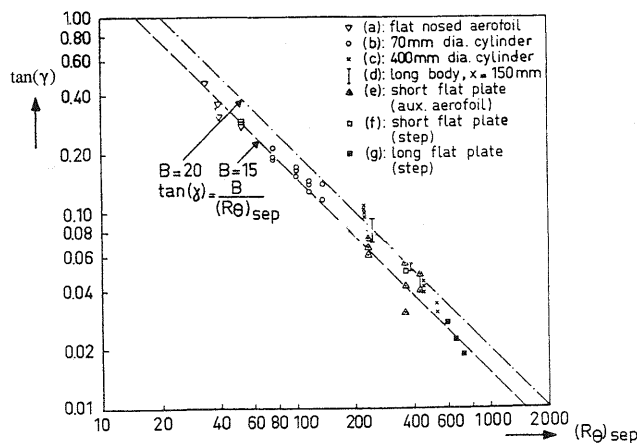


Fig. 5. Correlation between  $\tan(\gamma)$  and Reynolds number

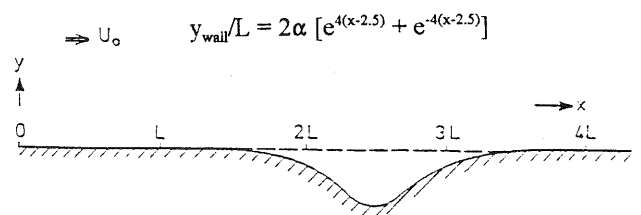


Fig. 6. Indented flat plate (CARTER and WORNOM)

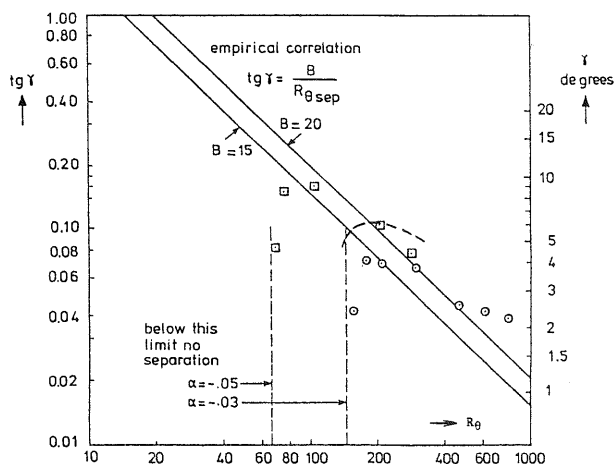


Fig. 7. Numerical results for indented plate.  $\odot$   $\alpha = -0.03$ ;  $\square$   $\alpha = -0.05$ ; - - - one parameter method for  $\alpha = -0.03$

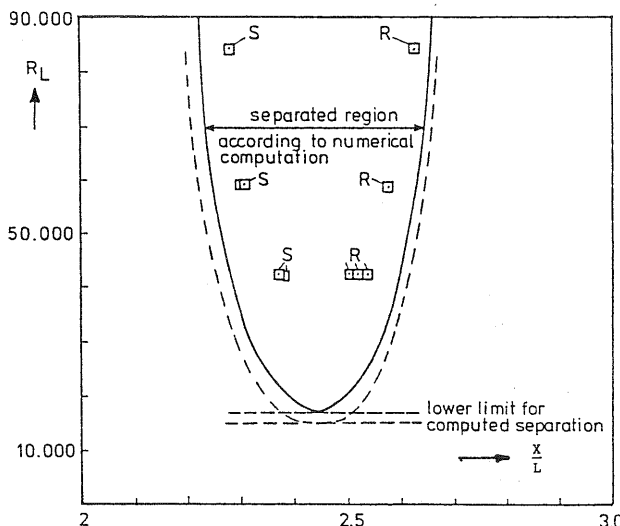


Fig. 8. Indented plate; theory and experiment. S = separation, R = reattachment;  $\square$  experiment; — finite difference method; - - - one parameter method

account using thin airfoil theory. Through the displacement thickness the Reynolds number has an effect on the separation bubble. When the Reynolds number is sufficiently decreased, the displacement thickness becomes so large that the boundary layer fills the dip in the surface to such an extent that the separation bubble disappears. Some results of Henkes' calculations are shown in Fig. 7. There appears to be some correspondence to our earlier experiments, except for the sudden disappearance of the bubble at low Reynolds numbers. In the experiments we always tried to obtain bubbles where the separation angle could be measured with some accuracy. Smoke pictures have been obtained for an experimental realization of a Carter and Wornom trough for  $\alpha = -0.03$ . Since the quality of these pictures is not sufficient for reproduction, only a comparison between experimental results and some calculations is shown in Fig. 8. A more recent computation by MEULEMAN [19] has shown that part of the discrepancy between experiment and finite difference calculation is due to the fact that the external pressure gradient in the experiment was not sufficiently equal to zero as assumed in the calculation. Also shown in Fig. 8 is the result of a calculation with a one parameter method. At present a two-parameter method is being developed which is based on the Hartree-Stewartson closure relations, supplemented by the finite difference results of HENKES [18] and MEULEMAN [19].

### 5. The $e^n$ method for transition prediction

For airfoil design and analysis one has to be able to predict the position of laminar-turbulent transition. In addition the characteristics of the initial turbulent boundary layer have to be known to be able to proceed with the boundary layer calculation. There are many empirical methods known to predict the position of transition of which the  $e^n$  method, based on linear stability theory, is at present the best known. This method was introduced 40 years ago independently by A. M. O. SMITH and the present author. Further developments have been made by many researchers, extending it to higher speeds, three-dimensional flows and including the effects of suction and heat transfer. That the method is still being used, is on the one hand due to the inherent difficulties of transition prediction from first principles. On the other hand, the  $e^n$  method contains enough physics to allow it to "predict" the distance to transition with only a simple experimental calibration. It was realized from the beginning that not enough physics was included to predict the process of transition itself. Hence providing the characteristics of the initial turbulent boundary layer remains a difficult problem of turbulence modelling (see section 8).

Reference [20] gives a recent review of various aspects of transitional boundary layers in aeronautics. Included in this volume is a paper by the present author [21] giving a detailed account of the historical development of the  $e^n$  method. Two other papers in [20] have been provided by authors from our group [22, 23]. The remaining part of this chapter gives a brief summary of [21], which should be consulted for detailed references to the literature cited.

From the end of the 19th century to about 1940 linear stability theory had been developed by a large number of mathematicians and theoretical aerodynamicists. Only through the famous experiments by SCHUBAUER and SKRAMSTAD it was shown that indeed "Tollmien-Schlichting waves" existed (the experiments were done in the period 1940-1945, but due to the war conditions the results became only widely known in 1948). Although PRETSCH had already done some amplification calculations, the results of which were presented in charts, it was only in the fifties that it was realized that linear stability theory might be used to bridge the sometimes large distance between the point of first instability and real transition.

It is difficult to specify the initial disturbances from which to start the amplification calculations. In fact this remains an important issue. How are disturbances generated inside the boundary layer? How are they related to outside disturbances like free stream turbulence, noise and vibration of the surface? At present this problem is denoted as “receptivity”. Therefore we have to be satisfied with the calculation of the ratio between the amplitude of the most amplified disturbance according to linear theory at the experimental transition position and the original amplitude of this disturbance at its neutral position. From SMITH’s analysis it turned out that in many cases the same amplification ratio of about  $e^9$  was found. The present author considered some of his own transition experiments on an EC 1440 airfoil. Guided by the flat plate experiment of SCHUBAUER and SKRAMSTAD this led him to conclude that beginning and end of the transition region correspond to amplification ratios of  $e^{7.8}$  and  $e^{10}$  respectively. On airfoils the transition region is in most cases only a few percent chord in length. Therefore it is not surprising that SMITH, putting much emphasis on his results for airfoils, had concluded to a mean value of  $e^9$ . The exponent 9 was very close to the mean value indicated by VAN INGEN. The early publications on this subject are [24–27].

Some of the results which the present author produced for the EC 1440 airfoil, making use of the Pretsch charts, are collected in Fig. 9. It should be noted that the factors 7.8 and 10 do not provide a very precise prediction of the transition region. This may have been caused by the fact that the laminar boundary layer was calculated by the Pohlhausen method which is known to be inaccurate near laminar separation. From Fig. 9 it follows that at the higher angles of attack transition occurs near or sometimes even downstream of laminar separation. Stability calculations were not available for separated flows (and hence Pretsch charts had to be extrapolated) and also the Pohlhausen method could not predict separated flows. It should also be realized that only later the possible existence of laminar separation bubbles was realized.

In his Ph.D. thesis, VAN INGEN [28] demonstrated that the  $e^9$  method could also be used for the case of porous suction. An extensive series of windtunnel measurements was done (using filtering paper as a porous surface). It should be emphasized that each time one of the components in the whole  $e^n$  method is changed (new boundary layer calculation method, new database for the stability diagrams, possibly improved stability diagrams, new experiments in the same or a different windtunnel, or flight tests) the whole method will have to be recalibrated. In this way the present author had come up in 1965 with  $n$ -factors of 9.2 and 11.2 for the beginning and end of the transition region for the same EC 1440 results as in Fig. 9. It cannot be overemphasized that the  $n$ -factor is not a magic number. It is just a convenient way to correlate into one single number a series of factors which are known from experiment to influence transition. The success of the method is due to the fact that an appreciable fraction of the distance between the point of instability and transition is covered by linear theory.

In 1966 the present author started to be involved in the design of airfoil sections for 2-D incompressible flows. The foundation of this work was laid while spending a sabbatical year at the Lockheed Georgia Research Laboratory. The then available numerical methods for conformal transformation, laminar and turbulent boundary layer calculation, and the  $e^n$  transition prediction method were used [29]. Later in Delft these design methods were continuously improved, based on comparisons between calculations and windtunnel tests. A large number of airfoil designs were made (especially by BOERMANS) and applied in many different sailplanes [30–34]. It was soon realized that at the chord Reynolds numbers applicable to sailplanes (and also windturbines) the occurrence of laminar separation bubbles was very important and warranted extensive research (see sections 4 and 7).

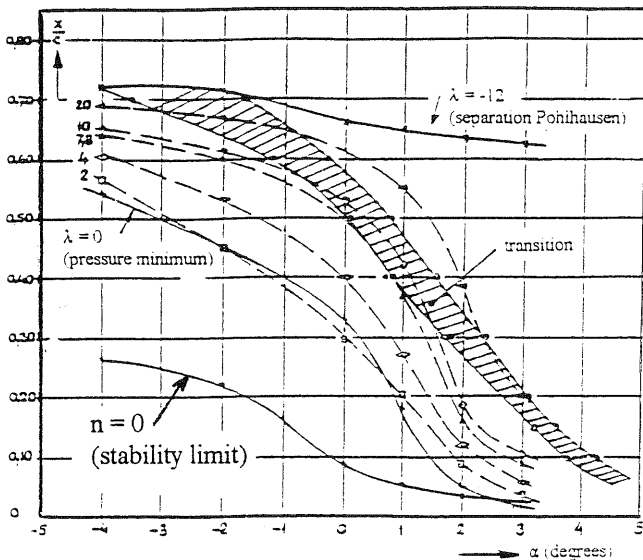


Fig. 9. Calculated  $n$ -factors and measured transition region for EC1440 airfoil section (VAN INGEN, 1956)

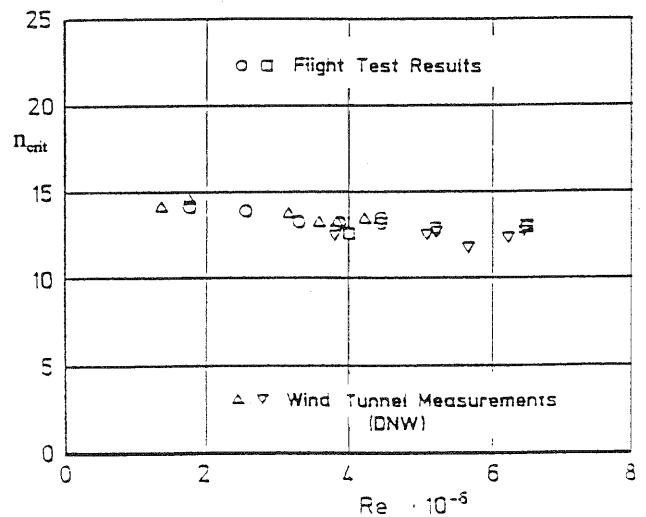


Fig. 10.  $n$ -factors at transition in flight and in the DNW-wind-tunnel

The  $e^n$  method could be extended to separated flows [9] because stability diagrams had been made available by TAGHAVI and WAZZAN for the Stewartson reversed flow solutions of the Falkner-Skan equation. Moreover improved stability calculations for the Falkner-Skan velocity profiles had been published by WAZZAN, OKAMURA, and SMITH and by KÜMMERER.

In the sixties it had been realized already for quite some time that a constant  $n$  factor could no longer be used. That for so long a constant  $n$ -factor of 9 had been useful, may have been due to the fact that most modern low speed, low turbulence windtunnels had been built according to the same recipe, aiming at a turbulence level of just below 0.1% as had been suggested to be sufficiently low according to the Schubauer and Skramstad experiment. From this experiment it had been concluded that reducing the turbulence level  $Tu$  below 0.1% had no use because "transition would not be influenced by a reduction of  $Tu$  below 0.1%". Since a further reduction of  $Tu$  requires a larger contraction ratio or more screens (and hence more money) most modern low speed windtunnel designs have aimed at  $Tu = 0.1\%$ .

From an evaluation of various transition experiments on flat plates at various turbulence levels the critical  $n$ -factor needed to predict flat plate transition as a function of turbulence level could be derived. It should be clear that free-stream turbulence level alone is not sufficient to describe the disturbance environment. Information about the energy distribution across the frequency spectrum should also be available and in addition to turbulence the acoustic disturbances are important.

Therefore we can only specify an  $n$ -factor if an "effective  $Tu$ " is known. This effective turbulence level can only be defined through a comparison of measured transition positions with calculated amplification ratios. In fact it has become customary to define the quality of a windtunnel by stating its "critical  $n$ -factor".

It should be realized that the  $e^n$  method does not automatically lead to useful results. The airfoil designer should be aware of its shortcomings and should make a judicious choice of the  $n$ -factors to be used. A comparison between  $n$ -factors obtained in flight and in the DNW low speed windtunnel is given in Fig. 10 (taken from HORSTMANN et al. [35]).

In the author's group L. M. M. BOERMANS is the designer using the various calculation methods described above (see also section 9). He also has performed rather extensive windtunnel measurements and has evaluated many flight tests. A number of examples can be found in the references to his work. As an example, Fig. 11, taken from BOERMANS and BLOM [30], shows results of computations with the  $e^n$  method for wavy and smooth versions of the same nominal airfoil. It follows that the  $e^n$  method is capable of predicting the shift in transition position due to waves in the surface. Fig. 12 gives the  $n$ -factor for the beginning of transition on the airfoil DU89-122 (tests in the low turbulence tunnel at Delft, using the infrared imaging technique, BOERMANS, private communication).

In the past decades the  $e^n$  method has established itself as a useful method to predict the distance to transition in 2-D incompressible flow. Apparently the linear stability theory has enough physics in it to account for the effects of pressure gradient, suction, heating and cooling, etc. on transition.

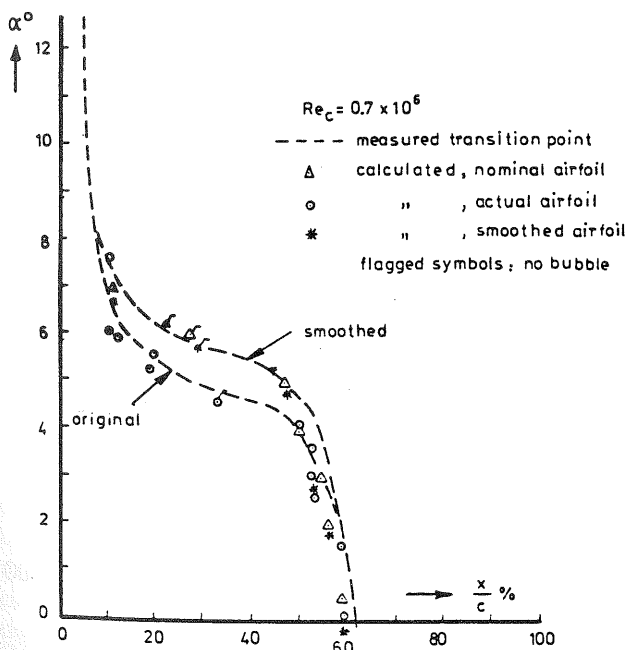


Fig. 11. Experimental and computed transition positions for "wavy" M-300 airfoil

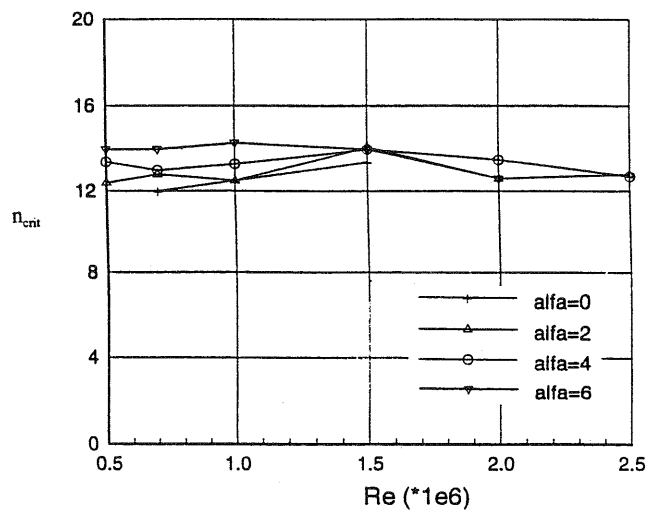


Fig. 12. Critical  $n$ -factors for the DU89-122 airfoil

6. Some further experimental results on the physics of transition

Although the  $e^n$  method gives us a reasonably accurate prediction of the position of transition for design purposes, it does not describe the physics of transition. Neither does it provide us with the characteristics of the turbulent boundary layer after transition, which would enable us to start a turbulent boundary layer calculation. This forces us to do more experimental and theoretical research on the physics of transition and turbulence modelling for the early stages of the turbulent boundary layer.

The present section summarizes some of the recent experimental research on laminar-turbulent transition done in our group. The text of this section is based on the recent Ph.D. thesis by VAN HEST [36]. It was mentioned already in section 5 that for boundary layer flows with a low external turbulence level, transition is introduced by Tollmien-Schlichting waves which, for a relatively large distance downstream of the first occurrence of instability, are well described by linear stability theory. Further downstream non-linearities occur and break-down of the unstable boundary layer occurs through the formation of three-dimensional turbulent spots. The existence of such turbulent spots has been described for the first time by EMMONS (1951). Early experimental studies have been performed by SCHUBAUER and KLEBANOFF (1955); they investigated natural turbulent spots as well as artificially triggered spots using an electric spark. Some of these earlier developments have been described by VAN HEST [36]. Most of the early studies of turbulent spots have been done in zero pressure gradient flow. The research of VAN HEST has been devoted to natural and triggered turbulent spots in relatively strong adverse pressure gradients.

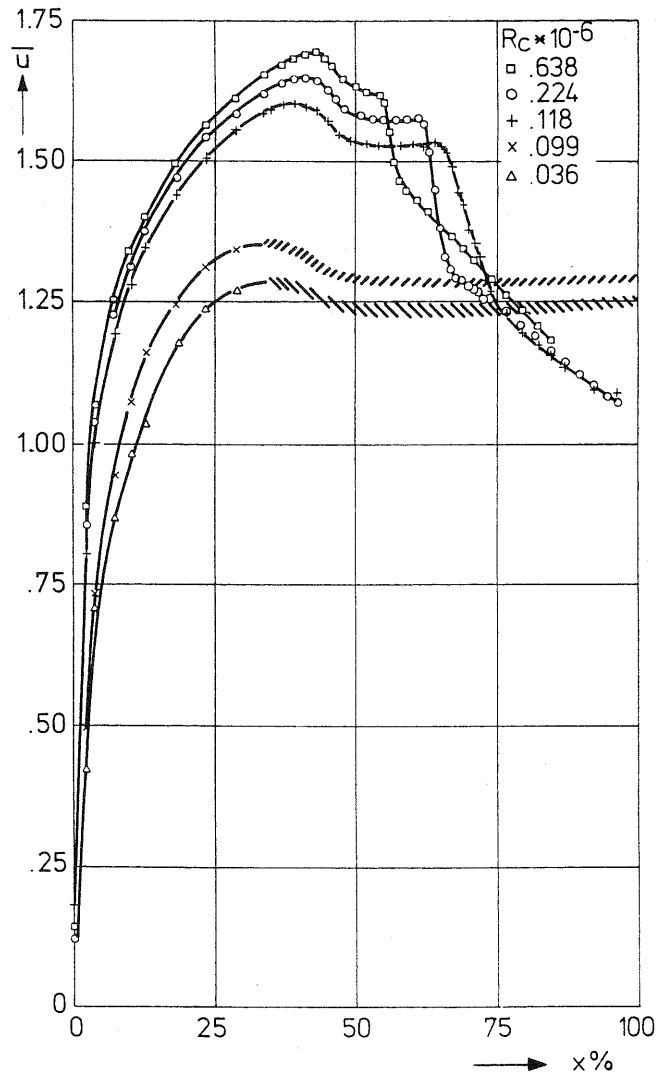
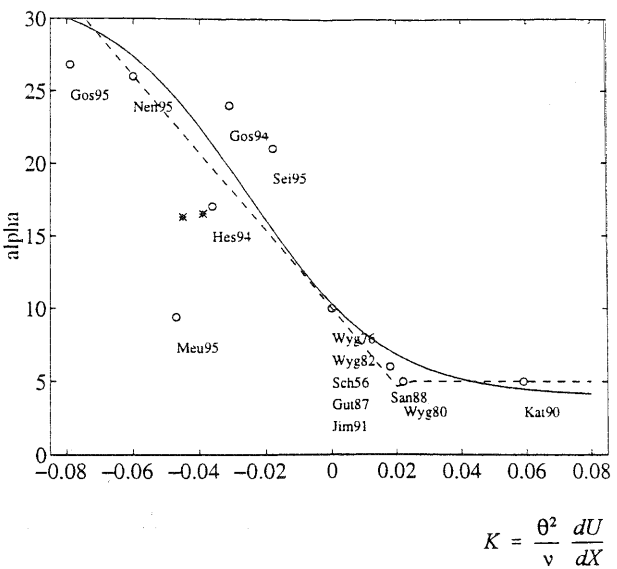
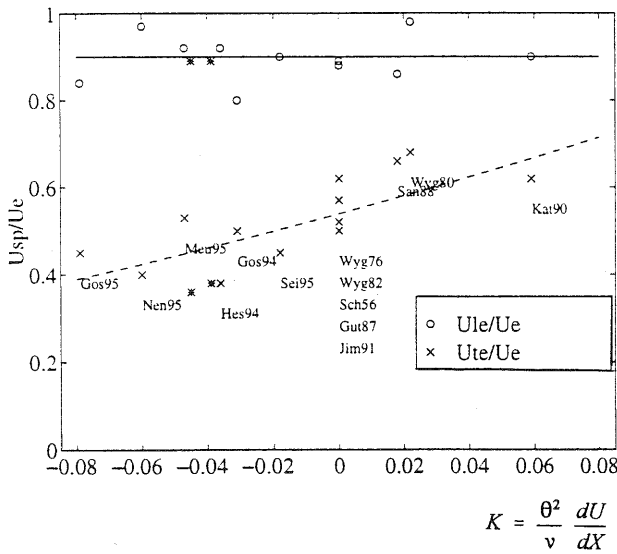


Fig. 13. Growth rates of triggered turbulent spots as function of the local pressure gradient parameter  $(\theta^2/\nu) (dU/dx)$  at transition. Top: leading and trailing-edge velocity. Bottom: spreading angle

Fig. 14. Pressure distribution for FX66-S-196V1 airfoil at various Reynolds numbers

Besides the physical processes in and around the spots the growth rates of the spots, as a function of the adverse pressure gradient are of interest, because any engineering calculation method to cover the region between fully laminar and fully turbulent flow must be based on these growth rates. The spots have a characteristic more or less triangular shape; they grow both in streamwise and spanwise direction until at a certain streamwise position they have merged into a completely turbulent flow.

The experiments with triggered spots were done in a small windtunnel with one flat wall on which the flow was studied and an opposite wall which could be adjusted to obtain the desired pressure distribution. The pressure distribution was chosen according to a Hartree similar flow with constant  $\beta$ . Turbulent spots were triggered by means of a pulsed pressure disturbance generated by a loudspeaker, mounted outside a hole in the test wall. Details of the flow were investigated using hot-wire anemometry. The reader is referred to VAN HEST [36] for a detailed description of the experiments including the data acquisition and processing technique. This reference may also be consulted for the details on the physical aspects of single and multiple interacting spots. Fig. 13 shows some results for the growth of triggered spots in streamwise and spanwise direction. A large influence of the adverse pressure gradient on growth rate is obvious. Also a tendency to relaminarization seems to be present at very strong favourable pressure gradients. From his experiments VAN HEST has derived improved correlations for the growth rates, as a function of the pressure gradient parameter.

A second series of experiments described by VAN HEST [36] is related to naturally occurring turbulent spots. In this case it is, of course, much more difficult to obtain detailed characteristics of the spots. It is not known beforehand when and where a spot will be formed! The experiments were done in the large boundary layer channel of our laboratory. Again a constant  $\beta$  Hartree flow was aimed at. Detailed comparisons between the experimental results and linear stability theory have been made. These comparisons confirm the observation, made in section 5, that for a relatively long distance downstream of the first occurrence of instability the linear theory gives a good description of the actual development of the disturbances.

Although there are differences between the shape of natural and triggered turbulent spots, there appears to be sufficient similarity to use the results for triggered spots for modelling the transitional region to be used in airfoil design codes. A special chapter in [36] is devoted to transition region modelling in which van Hest compares his results and correlations for spot growth rates, transition length, intermittency distributions, etc. with those of previous investigations. The present results will be used in our group to improve our airfoil design code (section 9).

## 7. Some further results on separation bubbles

In earlier sections of this paper we discussed the laminar part of separation bubbles. It is in principle possible to calculate fully laminar separation bubbles for arbitrary outside flows with either a full numerical approach or using the method of integral relations (preferably a two-parameter method). In practice however, the separated flow becomes highly unstable such that transition occurs in the separated flow. In general turbulent reattachment occurs, leading to a closed bubble. Sometimes the turbulent flow fails to reattach ("bubble bursting") with very large detrimental effects on lift and drag of airfoils. Even a closed separation bubble may have a large adverse effect on the drag of an airfoil due to the bad characteristics of the turbulent flow just downstream of reattachment. Therefore in our airfoil designs transition is triggered sufficiently far upstream to avoid these adverse effects (see section 9).

Although the  $e^n$  method is able to predict with reasonable approximation the transition position in the bubble, the prediction of whether reattachment does or does not occur is still a difficult task. Therefore extensive experimental research on separation bubbles has been done in our group at Delft. From this research a practical calculation method has been derived (VAN INGEN [9]). This topic will be illustrated with some figures and a brief comment. Fig. 14 shows the pressure distribution on a Wortmann airfoil for various decreasing values of the chord-Reynolds-number. Observe the flattened part of the pressure distribution in the separated area and compare this to the schematic description in Fig. 2. Below  $R = 118000$  bursting of the bubble occurs, leading to a drastic modification of the pressure distribution. The transition position in the bubble is predicted using the  $e^n$  method (section 5).

Various empirical criteria for bubble bursting are known from the literature (GASTER, CRABTREE, HORTON). In our airfoil analysis and design method we use a STRATFORD (1959) limiting pressure distribution downstream of the transition point T, to discriminate between reattaching and non-reattaching flows (Fig. 15). As soon as the Stratford curve does no longer intersect the basic pressure distribution, which would occur in absence of the bubble, bubble bursting is assumed to occur. It has been found that the resulting method represents, with a reasonable accuracy the results of the earlier empirical criteria. An improved method could be developed where the two-parameter method for the laminar part is supplemented with a simple turbulence model to which a switch is made at point T, resulting from the  $e^n$  method. Such improved methods should give a continuous changeover to the fully attached and fully developed turbulent boundary layer downstream of the bubble. Part of the research on turbulence modelling in our group is aimed at this particular region (see section 8).

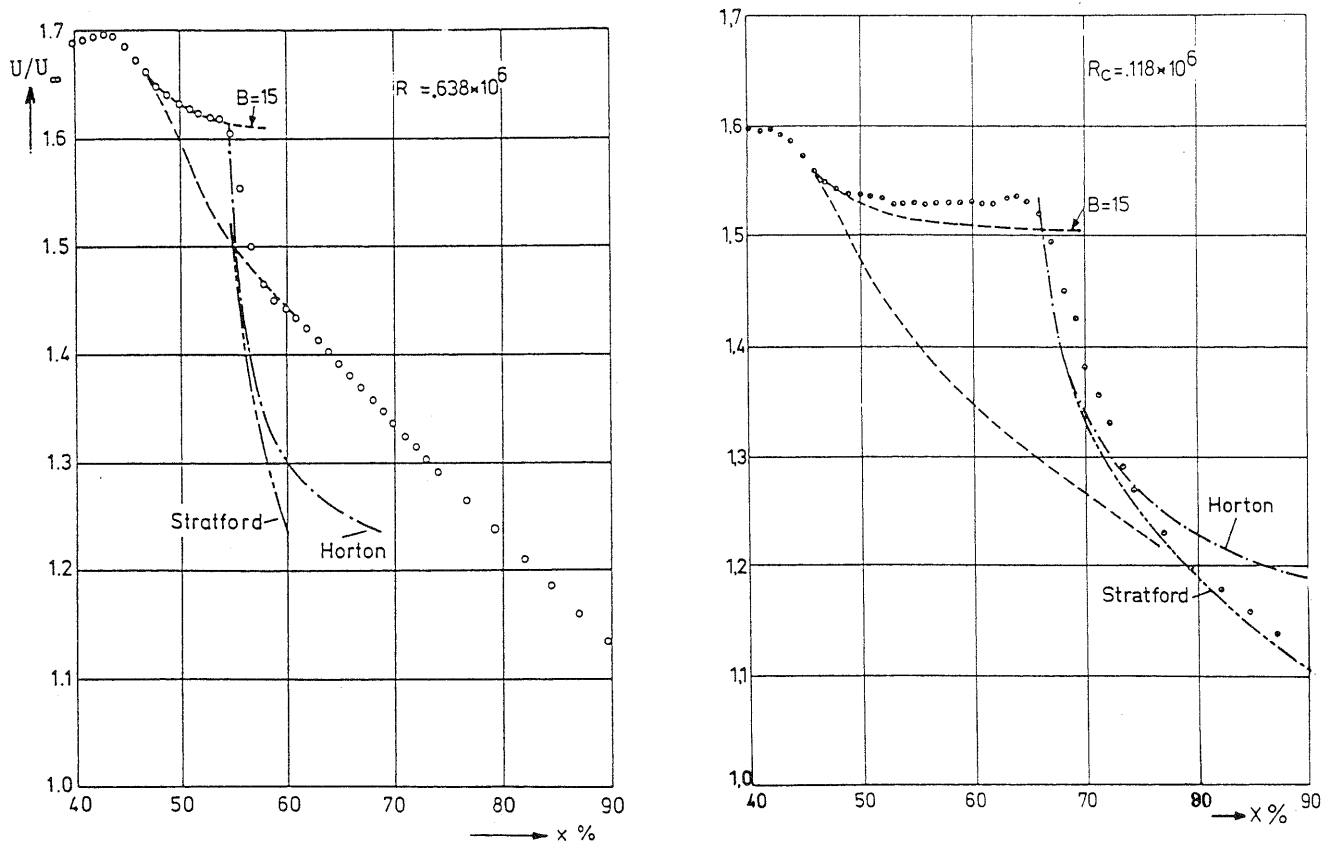


Fig. 15. Prediction of reattachment at two Reynolds numbers for the same airfoil as in Fig. 14

## 8. Turbulence modelling

For airfoil analysis and design it is a pre-requisite that the turbulent boundary layer and wake should be calculated with a reasonable accuracy. For "standard boundary layers" certain algebraic turbulence models may give acceptable results. However, in our airfoil work we have noticed that the turbulent flow in many cases does not behave in a "standard" way. In all cases providing the initial conditions for the turbulent boundary layer calculation downstream of transition remains a problem. Although there are attempts to develop methods with a continuous changeover from laminar to turbulent flow, using turbulence models which can represent laminar, transitional as well as turbulent boundary layers, such methods are not yet advanced to such a stage that they can be used in practical airfoil design. Our group contributes in various ways to the problem of turbulence modelling. HENKES [37] is working on the numerical aspects, PASSCHIER [38] is performing an experimental study on the characteristics of the turbulent boundary layer directly downstream of laminar separation. ABSIL [39] has investigated the flow in the vicinity of the trailing-edge of an airfoil. TUMMERS [40] is investigating turbulent wakes in very strong adverse pressure gradients. STARKE [41] is investigating the effects of wake curvature on the turbulence characteristics. Subsequent sections of the present chapter will give some highlights of this research. Further details can be found in the references.

In any CFD code for airfoil analysis and design the trailing-edge region should be given special attention. It is here that small details may have a large effect on lift through the viscous Kutta condition. It should be remembered that in airfoil theory, even if so-called inviscid, viscous effects at the trailing-edge play an important role. The well-known Kutta condition states that the (assumed) inviscid flow should leave the trailing-edge smoothly. It is often forgotten that this condition is based on a viscous argument, a real viscous flow cannot flow around a sharp edge, however a mathematical inviscid flow can. The implementation of the classical Kutta condition in inviscid flow is straight-forward and leads to a unique relation between angle of attack and circulation. However, what circulation should be chosen in an airfoil analysis and design code based on boundary layer methods is not at all obvious and requires extensive experimental research.

With this need in mind a long term research project has been performed in our group on the flow in the trailing-edge region of an NLR 7702 airfoil. A detailed discussion may be found in the Ph.D. thesis by ABSIL [39]. It should be clear that the flow near the trailing-edge is a very difficult case for modelling. The two boundary layers from the upper and lower surface merge at the trailing-edge. Because in our example the boundary layer on the upper surface is near to separation and that on the lower surface is far from separation, the near wake is highly asymmetrical. Within a very

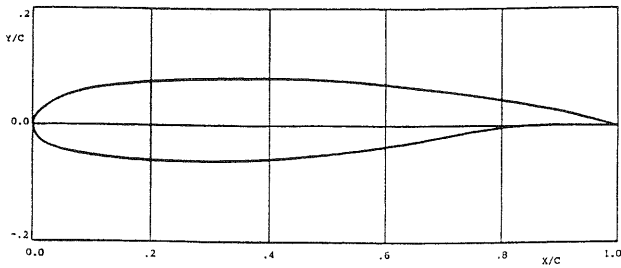


Fig. 16. The NLR 7702 airfoil

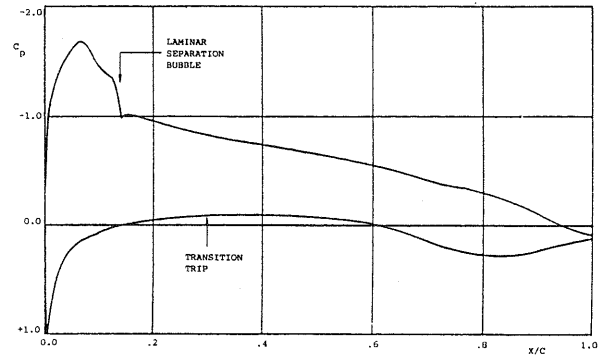


Fig. 17. Surface pressure distribution for NLR 7702;  $\alpha = 4^\circ$ ,  $Re = 1.5 \times 10^6$

short distance of a few percent chord the flow changes from the typical wall bounded case to the wake. Detailed experimental investigations were made using pressure probes, Preston tubes, hot-wire, and Laser-Doppler-Anemometry. In order to make the results useful for validation of computational methods, the utmost care was taken to ensure the accuracy and the self-consistency of the data set. All experiments were performed in the  $1.80 \text{ m} \times 1.25 \text{ m}$  low speed, low turbulence windtunnel in our laboratory. Fig. 16 shows the airfoil which was tested at fixed values of the angle of attack ( $4^\circ$ ) and Reynolds number ( $1.47 \times 10^6$ ). The resulting pressure distribution is shown in Fig. 17; the measurement grid is shown in Fig. 18. Note that boundary layer- and wake traverses overlap, which contributes to the check on the consistency of the data. Mean velocity vectors are shown in Fig. 19 and velocity profiles in the wake are given in Fig. 20. Note the extremely rapid change from the highly asymmetrical flow at the trailing-edge to a symmetric

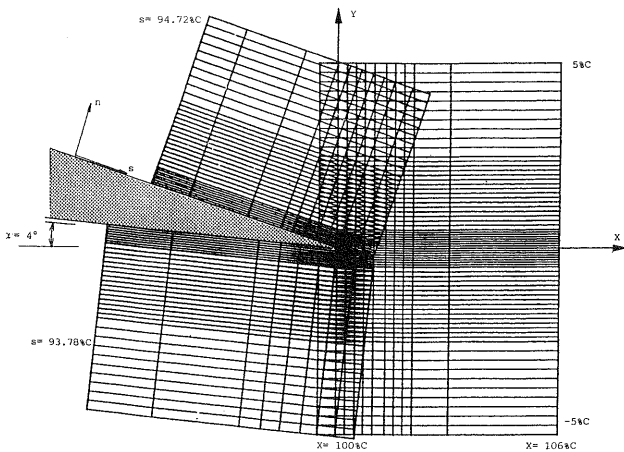


Fig. 18. The measurement grid for NLR 7702

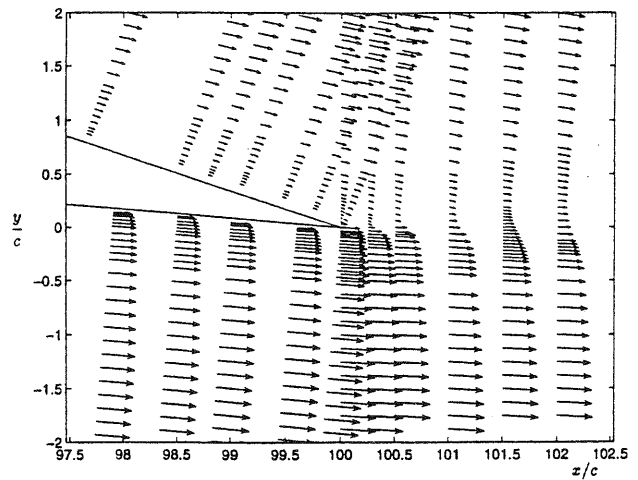


Fig. 19. Velocity vectors for NLR 7702

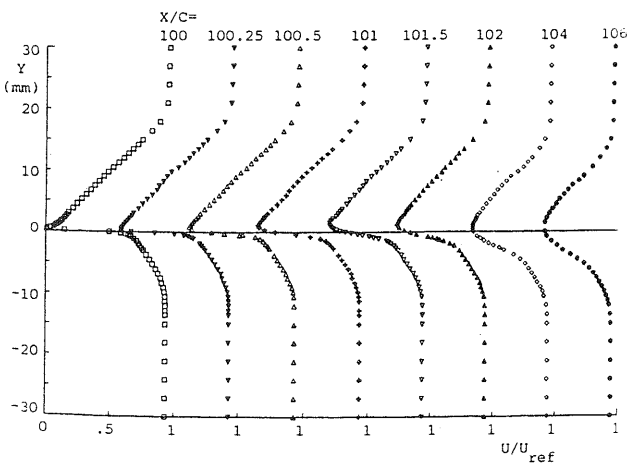


Fig. 20. Velocity profiles in the wake for NLR 7702

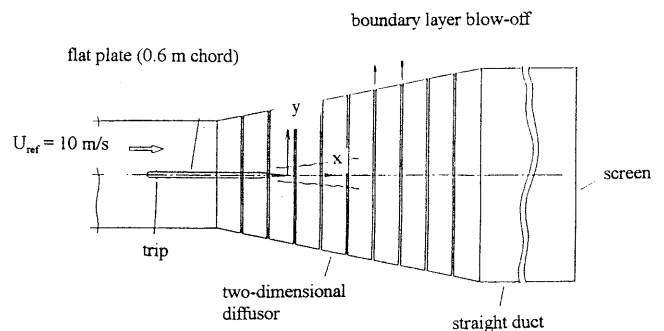


Fig. 21. Wake in adverse pressure gradient

wake. Also detailed results on various turbulent quantities have been obtained. Comparison with the usual algebraic turbulence models shows that a substantial modification of the empirical constants, as used in these models, would be required in order to represent the present flow.

In practice a wake, resulting from the main airfoil, may be subjected to a very strong adverse pressure gradient in the pressure field above a trailing-edge flap. It is not uncommon that flow reversal occurs in the centre of the wake. The strong adverse pressure gradient, in addition to the curvature of the wake and the high turbulence level in the wake make this flow a suitable candidate for turbulence research and turbulence modelling. Parts of this research have been published in [40]. A forthcoming Ph.D. thesis by TUMMERS [42] will give an extensive review of this research. For the present paper we have to be satisfied with presenting some highlights. Fig. 21 shows the experimental set-up. The wake is generated by a flat plate in the exit of a  $0.40\text{ m} \times 0.40\text{ m}$  windtunnel. The adverse pressure gradient is generated by a two-dimensional diffuser which is followed by a straight duct and a screen. Due to the screen the diffuser can be maintained at an overpressure with respect to the surroundings. Hence natural boundary layer blow-off occurs at the walls of the diffuser, contributing to the pressure gradient and at the same time preventing separation at the diffuser walls. Measurements were taken, using a three-component dual beam Laser-Doppler-Anemometry system. The development of the mean-velocity profile on the flat plate and in the wake follows from Fig. 22 ( $x = 0$  is at the trailing-edge of the plate). The centreline velocity is presented in Fig. 23, showing that flow reversal in the centre of the wake occurs at about 85 mm downstream of the trailing-edge of the flat plate. In addition to the mean velocity profiles detailed distributions of the Reynolds stresses and triple velocity correlations were measured, thus providing the possibility for a check on the balance of the kinetic energy equation. Computational results have been obtained with various existing methods. It has been concluded that the spreading rate of the mean velocity profiles is predicted well, but that the prediction of the centreline mean velocity and kinetic energy distribution is poor.

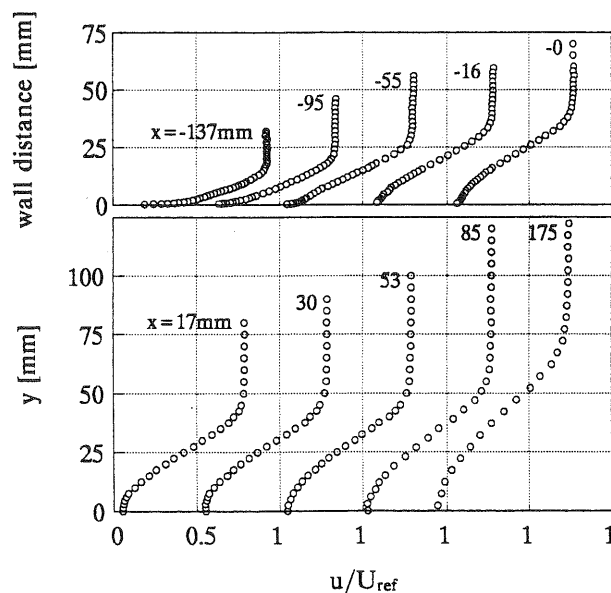


Fig. 22. Mean velocity profiles on the plate and in the wake

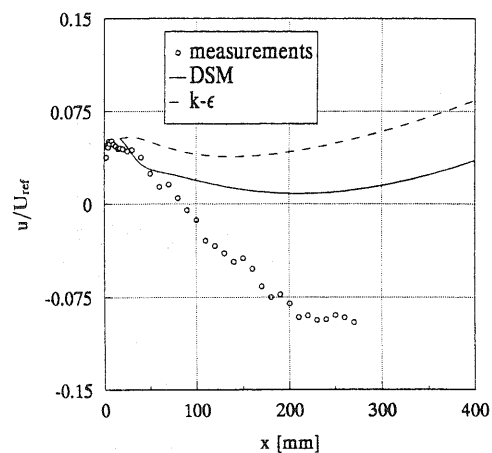


Fig. 23. Centre-line velocity in wake (calculations according to differential stress model and  $k - \epsilon$  model)

### 9. Some remarks on sailplane design at Delft University of Technology

As was stated already in the Introduction we at Delft try to combine fundamental research in aerodynamics with design activities. The sailplane provides an excellent link between the two activities. On the one hand airfoils can be tested at full scale Reynolds number in our moderately sized ( $1.25\text{ m} \times 1.80\text{ m}$ ) low turbulence, low speed windtunnel. On the other hand, through contacts with the sailplane industry, designs made at Delft, could be realized in practice. In this way students with different interests (design- or more fundamentally oriented) could work together on projects. In our group L. M. M. BOERMANS is responsible for the design aspects of this subject. References to his work may be found in [30–34].

Our first project, in collaboration with Alexander Schleicher Segelflugzeugbau in Germany, was the modification of the wing of the ASW-19 sailplane which increased the maximum glide ratio from 37.5 to 41. At the flight Reynolds numbers for sailplanes it is possible through proper shaping of the airfoil to maintain very long regions of laminar flow. This leads in general to the occurrence of laminar separation bubbles which has inspired the research described in sections 4 and 7.

Fig. 24 gives an example of the distribution of the momentum loss thickness over the upper surface of the same airfoil as in Fig. 14 at various Reynolds numbers. In all cases transition occurs downstream of separation, leading to a

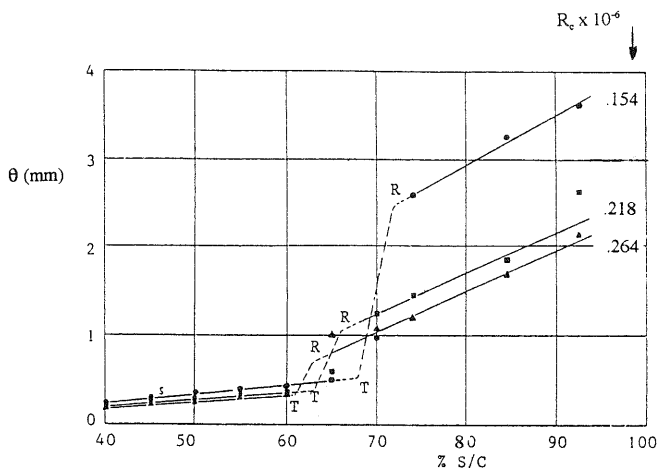


Fig. 24. Momentum-loss thickness for same airfoil as in Fig. 14

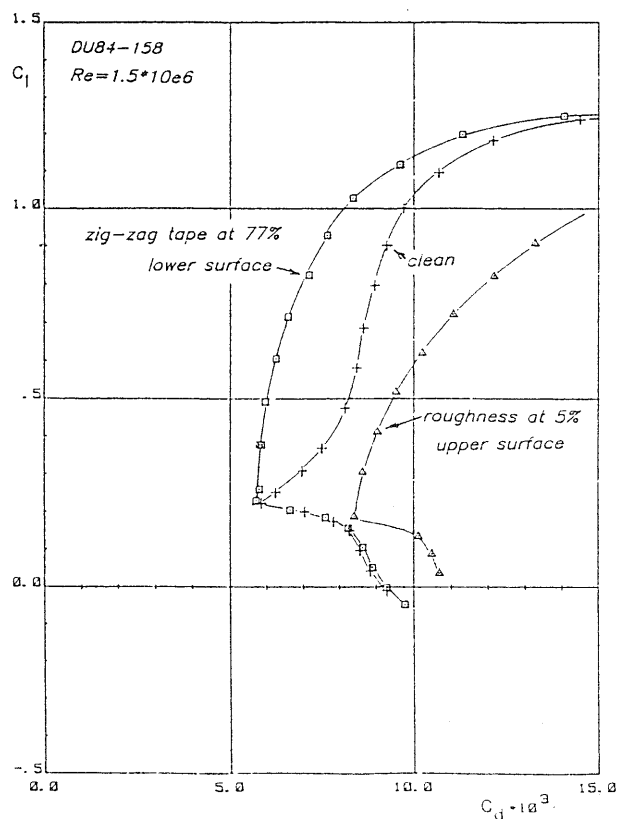


Fig. 25. Drag curves for airfoil DU84-158

laminar separation bubble. Note that at the lower Reynolds number there is a very strong increase of  $\theta$  between T and R, leading to a high value of  $\theta$  at the trailing-edge and hence to a large profile drag. Hence the designer should try to obtain long laminar flow regions but to avoid detrimental separation bubbles. This has led to the customary procedure to trip the boundary layer to the turbulent state at a short distance downstream of separation for which pneumatic turbulators are very often used. In this case air is blown out of the surface through a spanwise row of small holes; the blowing pressure is provided by a very small total head tube. As an example it can be mentioned that for the ASW-19 a tube diameter of 6 mm proved to be sufficient. Also the cheaper "zig-zag tapes" are used to trigger transition. It should be realized that the use of these boundary layer trips is only practicable if the airfoil is designed in such a way that laminar separation occurs at very nearly the same chordwise position for a range of angles of attack and of course the variable flight Reynolds numbers corresponding to the changing angles of attack. In practice, the zig-zag tape can become submerged in the laminar separation bubble, thus becoming ineffective, while pneumatic turbulators blow through the dead-air region and remain effective.

Fig. 25 shows the drag curves for the airfoil applied in the ASW-24 with and without the use of a zig-zag tape. The present state of the art is such that airfoils for sailplane applications can be designed which maintain laminar flow over 75% chord on the upper surface and 95% chord on the lower surface. A further improvement of the performance of such airfoils may only be achieved through the use of active boundary layer control such as suction. Our group is working on this subject. A further improvement of sailplane performance can be obtained by a better shaping of the fuselage and the wing-fuselage junction. A number of ideas from Delft have been incorporated in the design of the ASW-27 (Fig. 26). Fig. 27 shows one of the designs made in our group by BOERMANS. A prototype of a sailplane with a wing which is similar to the one shown in Fig. 27 is being built by Glasfaser Flugzeug Service, Germany.

The problem that led to the design of this prototype is the adverse effect of wing-fuselage interaction at increasing angles of attack. Due to the cross-flow around the fuselage the effective angle of attack ( $\alpha + \Delta\alpha$ ) of the airfoils near the fuselage increases more rapidly than the geometric angle of attack  $\alpha$ . This effect can easily be demonstrated by considering the cross-flow around an infinitely long circular cylinder. Fig. 28 shows  $\Delta\alpha/\alpha$  for the more complicated case of a midwing and various cambered shoulder wings for a fuselage with an elliptical cross section. The effect of the presence of the wing on the flow direction has been taken into account. It is obvious that a curved shoulder wing presents a great aerodynamic advantage. The resulting complications in the construction can be solved with modern materials such as carbon fibres.

The preceding examples show how challenging such projects may be for staff and students. Many of the techniques which have been developed for airfoil design are also being applied to the design of windturbine blades.

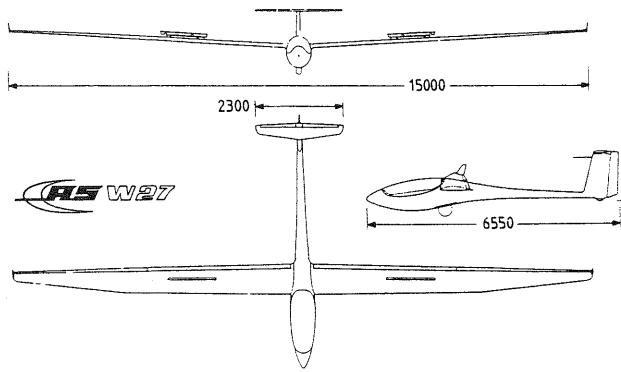


Fig. 26. The Schleicher ASW-27 sailplane

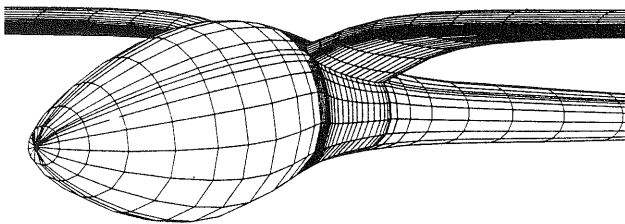
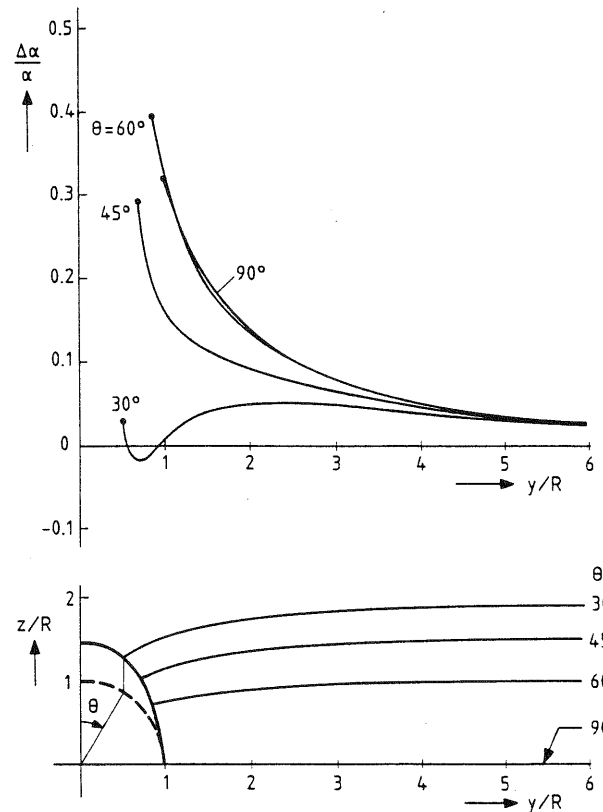


Fig. 27. Non planar wing-fuselage design

Fig. 28.  $\Delta\alpha/a$  for cambered shoulder wing and fuselage with elliptical cross section

## 10. Miscellaneous

In any paper, paying tribute to LUDWIG PRANDTL, the subjects of measuring techniques and flow visualization should not be missing. The final section of this paper will highlight a few examples from the Delft Low Speed Laboratory.

A well-known modern technique for visualizing transition from laminar to turbulent flow is the qualitative infrared thermography. Due to the difference in heat transfer from a surface in regions with laminar and turbulent flow, a temperature difference exists between the laminar and turbulent regions. This temperature difference can be visualized by means of a modern infrared camera. Even a quantitative representation of the temperature distribution along the surface can be obtained. This led us to the question whether the measured temperature distribution could be used to obtain quantitative information on the skin friction. The problem becomes easier when the temperature boundary layer remains thin as compared to the velocity boundary layer, because then the relation between skin friction and heat transfer ("Reynolds analogy") becomes tractable for arbitrary flows. This led to a technique where a small 3-D spot or a 2-D strip (through an oscillating mirror) is heated by a laser. When the laser is switched off the temperature distribution changes in time due to both diffusion of heat into the surface and to heat transfer to the flow. When the heat characteristics of the surface are known the heat transfer to the flow can be calculated by solving an equation for the temperature in the flowfield for various assumed local values of the skin-friction. By matching the calculated temperature distributions to the registrations obtained with the infrared camera, the proper value of the skin friction can be determined. Our Ph.D. student R. MAYER is working on this project; more information can be found in [43]. Fig. 29 gives some preliminary results of this research for a flat plate boundary layer in a small low speed wind tunnel. Observe that at very low speeds the result is not yet very accurate. This is thought to be due to the fact that the flat plate is placed in a vertical position so that free convection occurs which is not yet taken into account in the theory. However, the technique looks promising because it may be also expected that future generations of infrared cameras may be still more accurate.

The relation between the lift distribution on a 3-D wing and the vorticity field downstream is, of course, one of the subjects discussed already a long time ago by PRANDTL himself. Present-day measuring techniques and computer visualization of the test results are of interest, both in education and research. Fig. 30 and 31 give some results of our work; the figures should be self-explanatory. For more details see VELDHUIS [44].

Vortex flows are of course of much interest in relation to the generation of lift. For the validation of CFD codes experiments for flow configurations with stable vortices of sufficient size are useful. Therefore in our group much research has been done (by VERHAAGEN) on the vortex flows generated by sharp-edged deltawings [45–47]. As a tribute to PRANDTL, to whom already 70 years ago the generation of vortices apparently was of sufficient interest to make a flow visualization film, the present paper is closed with a recent vortex flow visualization (Fig. 32) by VERHAAGEN.

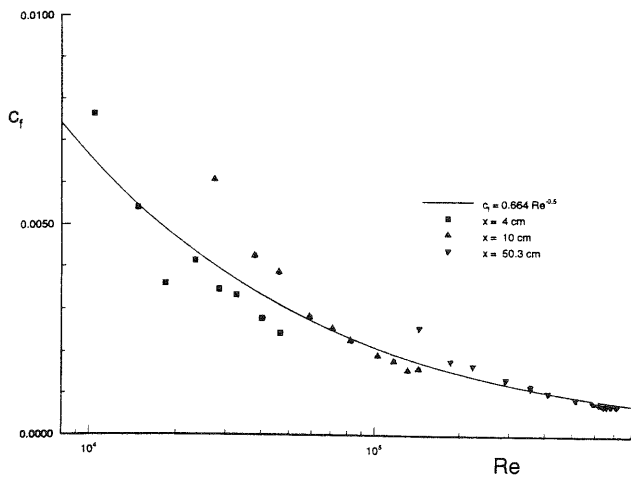


Fig. 29. Skin friction on flat plate determined from quantitative infrared thermography

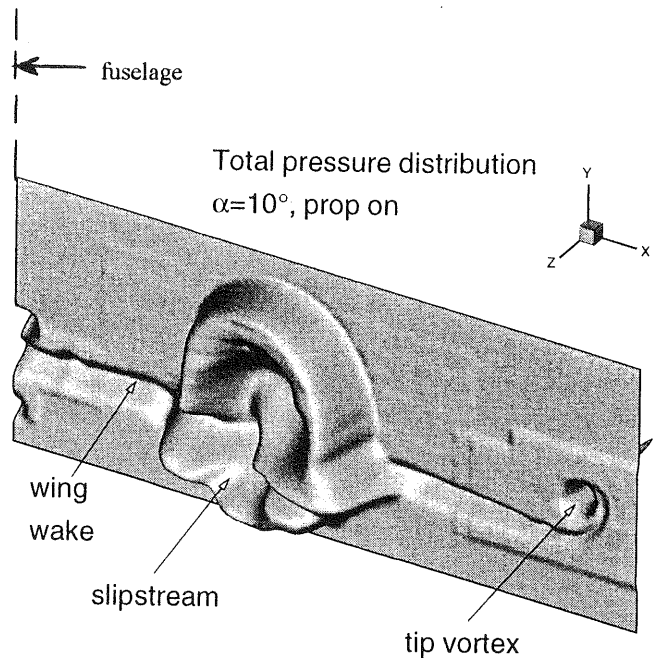


Fig. 30. Total pressure distribution behind propeller-wing combination

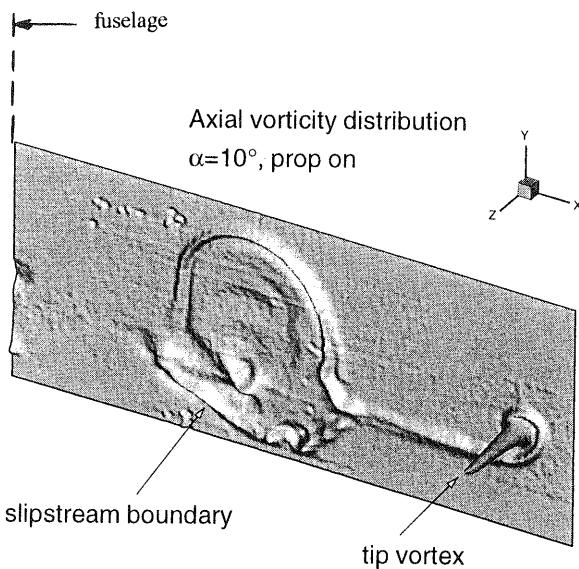


Fig. 31. Axial vorticity distribution behind propeller-wing combination

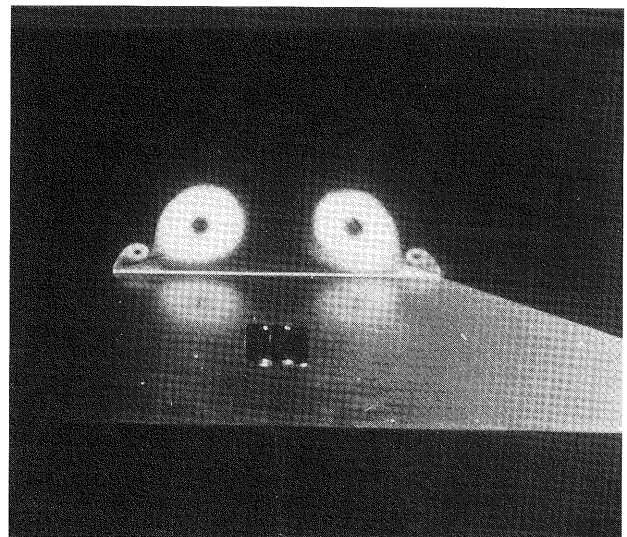


Fig. 32. Laser light-sheet flow visualization of vortices above a double delta wing

References

- 1 INGEN, J. L. VAN: Extended version of the Prandtl Memorial Lecture. To be published by the Faculty of Aerospace Eng., Delft University of Technology, 1997.
- 2 NIEUWSTADT, F. T. M.; STEKETEE, J. A. (eds.): Selected papers of J. M. Burgers. Kluwer Academic Publishers, Dordrecht/Boston/London 1995.
- 3 Anonymous: Description of the film "Production of vortices by bodies travelling in water". Rept. NLL A624, Year estimated at 1935.
- 4 PRANDTL, L.: The generation of vortices in fluids of small viscosity. Journal Roy. Aeron. Soc. (1927), 720.
- 5 PRANDTL, L.: Vorführung eines hydrodynamischen Films. ZAMM 7 (1927), 426.
- 6 SCHLICHTING, H.: Boundary-layer theory. 7th edition. McGraw-Hill 1979.
- 7 ROSENHEAD, L.: Laminar boundary layers. The Clarendon Press 1963.
- 8 CURLE, N.: A two-parameter method for calculating the two-dimensional incompressible laminar boundary layer. Journal Royal Aeron. Soc. 71, 117-123.
- 9 INGEN, J. L. VAN: On the calculation of laminar separation bubbles in two-dimensional incompressible flow. AGARD CP-168, 1975.
- 10 DOBBINGA, E.; INGEN, J. L. VAN; KOOI, J. W.: Some research on two-dimensional laminar separation bubbles. AGARD CP-102, Lisbon 1972.

- 11 INGEN, J. L. VAN: Transition, pressure gradient, suction, separation and stability theory. AGARD CP-224, Copenhagen 1977.
- 12 INGEN, J. L. VAN; BOERMANS, L. M. M.: Aerodynamics at low Reynolds numbers: A review of theoretical and experimental research at Delft University of Technology. Paper no. 1 in Proceedings International Conference, R. Ae. Soc. London 1986.
- 13 INGEN, J. L. VAN: Research on laminar separation bubbles at Delft University of Technology. pp. 537–556. In: KOZLOV, V. V.; DOVGAL, A. V. (eds.): Separated flows and jets. IUTAM Symposium, Novosibirsk, Springer 1990.
- 14 LEGENDRE, R.: Decollement laminaire regulier. *Comptes Rendus* **241** (1995), 732–734.
- 15 OSWATITSCH, K.: Die Ablösungsbedingung von Grenzschichten. In: Grenzschichtforschung/Boundary layer Research. IUTAM Symposium Freiburg/Br. 1957; Springer Verlag 1958, pp. 357–367.
- 16 VELDMAN, A. E. P.: New quasi-simultaneous method to calculate interacting boundary layers. *AIAA Journal* **19** (1981), 79–85.
- 17 CARTER, J. E.; WORNOM, S. F.: Solutions for incompressible separated boundary layers including viscous-inviscid interaction. Aerodynamic analyses requiring advanced computers. Part 1. NASA SP 347, pp. 125–150, 1975.
- 18 HENKES, R. A. W. M.; VELDMAN, A. E. P.: On the breakdown of the steady and unsteady interacting boundary-layer description. *J. Fluid Mech.* **179** (1987), 513–529.
- 19 MEULEMAN, C. H. J.: Computation of laminar separation bubbles in boundary layers with a streamwise pressure gradient. Engineering Thesis, Delft University of Technology, Faculty of Aerospace Engineering 1996.
- 20 HENKES, R. A. W. M.; INGEN, J. L. VAN (eds.): Transitional Boundary Layers in Aeronautics. Proceedings of the Colloquium; organised by the Royal Netherlands Academy of Sciences, Section Physics, Part 46. North-Holland, Amsterdam/Oxford/New York/Tokyo 1996 (ISBN 0-444-85812-1).
- 21 INGEN, J. L. VAN: Some introductory remarks on transition prediction methods based on linear stability theory. In [20], pp. 209–224.
- 22 HENKES, R. A. W. M.: Colloquium on transitional boundary layers in aeronautics. Background, summary and discussion. In [20], pp. 3–30.
- 23 HEST, B. F. A. VAN; GROENEN, H. F.; PASSCHIER, D. M.: Nonlinear development and breakdown of TS-waves in an adverse pressure gradient boundary layer. In [20], pp. 71–79.
- 24 SMITH, A. M. O.; GAMBERONI, N.: Transition, pressure gradient and stability theory. Report ES 26388, Douglas Aircraft Co. 1956.
- 25 SMITH, A. M. O.: Transition, pressure gradient and stability theory. Proc. 9th Int. Congress Appl. Mech., Brussels 4, pp. 234–244.
- 26 INGEN, J. L. VAN: A suggested semi-empirical method for the calculation of the boundary layer transition region. Rept. VTH74, Dept. Aeron. Eng., Delft (extended version in Dutch in Rept. VTH-71) 1956.
- 27 INGEN, J. L. VAN: A suggested semi-empirical method for the calculation of the boundary layer transition region. Proc. Second European Aeronautical Congress, Scheveningen 1956, pp. 37.1–37.6.
- 28 INGEN, J. L. VAN: Theoretical and experimental investigation of incompressible laminar boundary layers with and without suction. Rept. VTH-124, Delft University of Technology, Dept. of Aerospace Engineering 1965.
- 29 INGEN, J. L. VAN: Advanced computer technology in aerodynamics: a program for airfoil section design utilizing computer graphics. AGARD Lecture Series 37. High Reynolds-number subsonic aerodynamics, pp. 8.1–8.33.
- 30 BOERMANS, L. M. M.; BLOM, J. J. H.: Low speed aerodynamic characteristics of an 18% thick airfoil section designed for the all-flying tailplane of the M-300 sailplane. Rept. LR226, Fac. Aerospace Eng., Delft 1976.
- 31 BOERMANS, L. M. M.; SELEN, H. J. W.: Design and tests of airfoils for sailplanes with an application to the ASW-19B. ICAS-Paper 82-5.5.2., 1982.
- 32 BOERMANS, L. M. M.; WAIBEL, G.: Aerodynamic and structural design of the Standard Class sailplane ASW-24. ICAS-Paper 88-2.7.2., 1988.
- 33 BOERMANS, L. M. M. et al.: Experimental aerodynamic characteristics of the airfoils LA5055 and DU86-084/18 at low Reynolds numbers. pp. 115–130. In: MUELLER, T. J. (ed.): Low Reynolds number aerodynamics. Proc. Conf. Notre Dame, 5–7 June 1989.
- 34 BOERMANS, L. M. M.; GARREL, A. VAN: Design and windtunnel test results of a flapped laminar flow airfoil for high-performance sailplane applications. ICAS 94-5.4.3., 1994.
- 35 HORSTMANN, K. H.; QUAST, A.; REDEKER, G.: Flight and wind-tunnel investigations on boundary layer transition. *J. Aircraft* **27** (1990), 146–150.
- 36 HEST, B. F. A. VAN: Laminar-turbulent transition in boundary layers with adverse pressure gradient. Ph.D. thesis, Technical University Delft 1996 (ISBN 90-5623-048-4).
- 37 HENKES, R. A. W. M.: Scaling of equilibrium boundary layers under adverse pressure gradient according to different turbulence models. Submitted to AIAA J., 1997.
- 38 PASSCHIER, D. M.: Hot wire measurements in the neighbourhood of a laminar separation bubble. To be published by the Faculty of Aerospace Engineering, Delft 1997.
- 39 ABSIL, L. H. J.: Analysis of the Laser Doppler measurement technique for application in turbulent flows. Ph.D. Thesis, Delft University of Technology 1995 (ISBN 90-5623-017-4).
- 40 TUMMERS, M. J.; PASSCHIER, D. M.; HENKES, R. A. W. M.: Experimental investigation of the wake of a flat plate in an adverse pressure gradient and comparison with calculations. Proc. 10th Symp. on Turbulent Shear Flows, University Park, U.S.A., August 14–16, 1995.
- 41 STARKE, A. R.; HENKES, R. A. W. M.; TUMMERS, M. J.: Experiments for the effects of curvature and pressure gradient on the turbulent wake of a flat plate. Proceedings of the 11th Symposium on Turbulent Shear Flows, France, 8–11 September 1997.
- 42 TUMMERS, M. J.: Investigation of an adverse pressure gradient wake using Laser Doppler anemometry. Ph.D. Thesis, Technical University Delft 1997.
- 43 MAYER, R.; HENKES, R. A. W. M.; VAN INGEN, J. L.: Wall-shear stress measurement with quantitative infrared thermography. Proceedings of Eurotherm Seminar, nr. 50, QIRT 96, Stuttgart 1996.
- 44 VELDHUIS, L. L. M.: Analysis of propeller slipstream effects on a trailing wing. ICAS-96-4.10.3, pp. 2392–2413.
- 45 VERHAAGEN, N. G.: An experimental investigation of the vortex flow over delta and double-delta wings at low speed. AGARD CP no. 342, Paper 7, Rotterdam, April 1983.
- 46 VERHAAGEN, N. G.; MEEDER, J. P.; VERHELST, J. M.: Boundary layer effects on the flow of a leading-edge vortex. AIAA Paper 93-3463-CP, Monterey, August 1993.
- 47 VERHAAGEN, N. G.; NAARDING, S. H. J.: Experimental and numerical investigation of the vortex flow over a sideslipping delta Wing. *J. of Aircraft* **26** (1989).

Received March 7, 1997

*Address:* Prof. Dr. Ir. J. L. VAN INGEN, Delft University of Technology, Faculty of Aerospace Engineering, Kluyverweg 1, 2629 HS Delft, The Netherlands (also participant in the J. M. Burgers Centre for Fluid Mechanics)